Technical Effects of Molecule-Electrode Contacts in Graphene-Based Molecular Junctions

Qian Zhang,[1,2] Shuhui Tao, [1,2] Yinqi Fan, [1,2] Cezhou Zhao,[3] Chun Zhao, [3] Weitao Su, [4] Yannick J. Dappe,[5] Richard J. Nichols,[2] Li Yang[1,2]*

1. Department of Chemistry, Xi'an-Jiaotong Liverpool University, Suzhou, China.

2. Department of Chemistry, University of Liverpool, Liverpool, UK.

3. Department of Electrical and Electronic Engineering, Xi'an-Jiaotong Liverpool University, Suzhou, China

4. College of Materials and Environmental Engineering, Hangzhou Dianzi University, 310018, Hangzhou, China

5. SPEC, CEA, CNRS, Université Paris-Saclay, CEA Saclay 91191 Gif-sur-Yvette Cedex, France

ABSTRACT

This study focuses on comparing methods for capturing and measuring the charge transport properties of single molecules in gold-graphene contact gaps. We have attempted to measure the single molecule conductance of a series of 1,n-alkanedithiols (n=4, 6, 8) tethered between a gold and a graphene contact with three different methods. The CP-AFM break junction (CP-AFM BJ), STM break junction (STM BJ) and STM based *I*(*s*) techniques for forming molecular junctions with graphene lower contacts were compared. In each case the upper contact was gold, with a gold coated AFM probe in the CP-AFM BJ method and a gold STM tip for both the STM BJ and *I*(*s*) techniques. Both the CP-AFM BJ and the STM based *I*(*s*) method yielded similar values for the conductance decay constant values, with β_N = 0.56 and 0.40, respectively. In line with previous observations, this is much smaller than values recorded for the same alkanedithiol series in symmetric gold-molecule-gold junctions where we find that β_N = 1.1. This clearly shows the impact of substituting one of the gold contacts for a graphene one. This observation has been previously rationalized as resulting from the breaking of junction symmetry, the change in electrode-molecule coupling and energy level alignment. On the other hand, stable molecular junctions could not be formed using the STM BJ technique with graphene contacts which may be due to transient instability in the gold tip contact after it has been pushed hard onto the graphene surface.

1.Introduction

Investigating the nature of charge transport through molecules tethered between pairs of electrode contacts is one of the most active areas of contemporary molecular electrodes.[1] A range of factors can influence the electrical characteristics of such molecular junctions, including the intrinsic properties of molecules and electrode materials, the external environment, the molecule-electrode binding or molecular orbitals alignment in relation to the Fermi levels of the electrodes.[2] To date, the most widely used techniques for probing the electrical properties of molecular junctions include mechanically controlled break junctions (MCBJ),[3] scanning tunneling microscopy based break junctions (STM-BJ), the *I*(*s*) technique,[4-5] and conducting probe atomic force microscopy (CP-AFM).[6-7] Originally introduced by Xu and Tao in 2003,[4] the STM break junctions (BJ) method creates in-situ a metallic gold-to-gold junction between the gold STM tip and the gold substrate in the presence of a solution of the target molecule or an adsorbed layer on the gold substrate. Upon withdrawal of the STM tip the metallic junction is cleaved leaving a gap into which the molecular target can adsorb and form a gold-molecule-gold junction. During the process of tip withdrawal, a conductance step near the so-called quantum conductance (G_o) is observed as the metallic contact is cleaved. This is followed on further tip retraction by a smaller conductance step as the molecular junction is subsequently broken. The tip is repeatedly cycled into and out of contact with the gold substrate and conductance histograms are recorded from many junction formation and breaking cycles to reveal peaks corresponding to the junction conductance.

Similar to the STM-BJ method, the *I*(*s*) technique[5] also employs an STM tip to form the molecular junctions which are also extended until they cleave. A similar procedure of repeatedly forming and breaking junctions is also followed and molecular conductance is also determined by statistical analysis and histogram construction from a large number of such traces. The key

difference between the STM-BJ and *I*(*s*) methods, lies in the fact that for the latter technique the tip is brought very close to the substrate surface, but direct metallic contact is avoided. As such the *I*(*s*) technique has been referred to as a "non-contact method". It is also worthwhile mentioning here the STM "Touch-to-Contact" method, in which the STM tip is positioned just in contact with the top of the molecular monolayer film. As described by Martin et al. the separation between the STM tip and substrate is determined through a calibration procedure which relates the STM set-point parameters to an absolute tip-substrate separation.[8] The STM "Touch-to-Contact" avoids both incursion of the tip into the molecular monolayer film or a gap between the top of the monolayer and the STM tip.

CP-AFM can also be used to determine the electrical characteristics of metal|molecule|metal junctions. Typically, the CP-AFM technique uses an AFM conducting probe to contact with a self-assembled molecular monolayer (SAM) on a metal substrate.[6] The AFM feedback loop controls the force loaded onto the surface while the current–voltage (I–V) relationship of the molecular layer sandwiched between the tip and surface is recorded. This is not a single molecule determination since the area probed depends on the tip geometry, contacting force and deformation properties of the monolayer, but typical conditions for self-assembled monolayers may result in tens or hundreds of molecules being contacted.[6] CP-AFM may also be used to probe single molecule junctions by using the technique developed by Cui and Lindsay[7,9] in which gold nanoparticles are adsorbed on-top of self-assembled molecular monolayers of monothiols containing a small concentration of dithiols, which electrically wire the nanoparticle to the surface. Touching the top of such gold nanoparticles with the CP-AFM tip then enables I-V characteristics of the molecular junction to be recorded.[9] Another way to form single molecule junctions by CP-AFM is the CP-AFM break junction (CP-AFM BJ) approach. In this method, the conducting AFM

tip is brought into contact with the surface covered by the molecular target. The AFM tip is then rapidly retracted while monitoring the current and force signals.[10-11] As for the STM-BJ and *I*(*s*) methods, during such formation and retraction cycles molecular junctions can be formed and cleaved and traces analyzed to extract single molecule data following a similar statistical analysis.

The techniques mentioned above share the basic concept of being able to capture single or small groups of molecules and recording electrical signals while the molecular junctions are stretched and broken. These techniques have been used to study many fundamental aspects of single molecule junctions and they have given new impetus to the field of molecular electronics. However, despite sharing the same basic concepts there is an ongoing debate on the comparability between these techniques in terms of single molecule conductance determination. Apparent discrepancies between conductance values have been reported between different laboratories using these different techniques. For example, in early studies the conductance of octanedithiol was measured to be 20 nS using the STM BJ technique by Xu *et al*.,[4] while Haiss *et al.* obtained a value of 1 nS by the analogous STM technique.[12] This was later rationalized as arising from different ways in which these alkanedithiols can bind to the gold contacts through the thiol end groups, with the differing techniques favoring different anchoring configurations.[13-16] Indeed, measurements on surfaces of different roughness showed different prominent conductance values.[14] Measurements with the STM-BJ technique tend to form "rougher" contacts due to the gold contact breaking while the *I*(*s*) technique can be applied to flat surface areas if desired. In this respect these techniques can be seen as complementary and application of both to the same molecular system could be expected to broaden the view of the molecular junction properties and spread of favoured junction conductance values. CP-AFM, on the other hand, conveys the advantage of being able to record the force and current signals simultaneously offering the possibility to correlate electrical and

mechanical properties of junctions.[2,17] However, a potential disadvantage can arise with the use of AFM tips with higher radii of curvature, where there could be ambiguity about forming truly single molecule junctions when CP-AFM is used to form break junctions. In any case, measurements of molecular conductance with several different techniques should be seen as advantageous.[17]

Metallic materials have been widely used as the electrodes to construct molecular junctions, where desired characteristics are outstanding stability, conductivity and fabricability.[18] There are indeed a plethora of investigations of molecular junctions using metals (Au, Ag, Pt, Al and Cu) as the electrodes.[19-20] However, there is an increasing interest in deploying carbon based electrodes to fabricate metal-free molecular junctions.[21] Among carbon-based materials, graphene is a promising material with remarkable electrical and structural properties. On account of its high structural stability, charge carrier mobility, high thermal conductivity and optical transmittance, graphene is considered to have many applications in electronics devices.[22] To date, systematic comparative investigations of graphene/molecule junctions formed by a variety of single molecule junction techniques have not been performed.

In light of the discussion above, we systematically investigate the molecular conductance with a bottom graphene contact by comparing resulting from the STM-BJ, STM *I*(*s*) and CP-AFM BJ techniques. As a first step, the conductance of 1,8 octanedithiol in gold-gold junctions was measured by the STM-BJ, *I*(*s*) and CP-AFM BJ techniques to provide control experiments and to evaluate the stability of our experimental setup. These data for Au-alkanedithiol-Au junctions corresponds well with the literature. Following this, the setups were applied to gold-graphene asymmetric junctions. The length dependence of conductance for Au/alkanedithiols/graphene junctions has been determined and decay constants (attenuation factors) compared. When compared to standard gold-gold junctions, a lower attenuation factor is observed for the gold-

graphene counterparts when applying both the STM-based *I*(*s*) and CP-AFM methods. On the other hand, stable molecular junctions using graphene bottom contacts could not be formed with the STM BJ method and reasons for this are suggested.

2.Methods

The compounds included in this study are 1,6 hexanedithiol, 1,8 octanedithiol and 1,10 decanedithiol, which were purchased from Alfa Aesar and used as received. The tips for the STM break junction were cut mechanically before use, while the tips for the *I*(*s*) technique were made by electrochemical etching of gold wires (0.25 mm, Tianjing Lucheng Metal company, 99.99%) following the method described by Ren *et al.*[23] The gold coated AFM tip was purchased from the Budget Sensors (Multi75GB-G) and used after calibration of the force constant and resonance frequency on the sapphire substrate. The bottom electrodes used were a few layers graphene and gold substrates, which are brought from the Graphene Supermarket (US) and Arrandee Gold (Germany), respectively. The gold substrate (1×1 cm) was annealed under a butane flame to generate an Au (111) microstructured surface before use in the experiments. For measurements performed in the liquid cell, mesitylene was used to form 1 mM solutions. The cell was cleaned in an ultrasonic bath in piranha solution (warning: handle with great care!) for 5 minutes followed by 5 minutes in an ultrasonic bath with ethanol/acetone solution. The distilled water used for rinsing was produced by an in-house water purification system.

The STM break junction technique. A modified STM system (based on Keysight Technology 5500) was used for the STM-BJ method. A mechanically cut Au tip was used to fabricate the gold-molecule-gold and gold-molecule-graphene molecular junctions. The gold/graphene substrate was mounted on the STM stage with the liquid cell. The gold tip was bought close to the surface at a

current of 0.015 nA with a bias voltage of 0.2 V during the tip approach. The current was then increased to 0.1 and then to 1 nA in a stepwise manner to check the stability. Finally, the current was set to 30 nA to create the metallic point contacts in the case of gold/gold junctions or hard gold/graphene contacts for the graphene experiments. The current-distance signals were recorded with an external data acquisition instrument. A Z-sweep could be applied to the scanner (Z sweep 4 nm, 0.3 per second) if the system became unstable to help to remove tip instabilities/contamination. The collected curves were then used for data analysis and histograms generation.

The STM based *I*(*s*) technique. This technique was implemented in accordance with methods first described by Haiss *et al.*[5] with necessary modification of our Bruker STM equipment. Details can be also found in our previous studies.[24-25] Briefly, the electrochemically etched Au tip (ethanol: HCl 37% = 1:1, voltage = 4 V) was set at an initial vertical distance (4 nm) and then advanced toward to the molecule-covered substrates. This displacement towards the surface was achieved by setting a preset threshold of the set-point current (10 nA). The STM tip was then retracted to its initial distance and this approach-retraction cycle was repeated continuously. During the process, the current and distance signals were collected for further data analysis to obtain the most probable conductance values. The conductance Au-1,8 octanedithiol-Au junctions was determined in the liquid cell, while the conductance of graphene-based junctions was measured under air condition.

The CP-AFM break junction technique. The Bruker Multimode 8 microscope equipped with a conductive AFM application module was used for formation of the molecular junctions by the CP-AFM BJ method. Such experiments were made under ambient conditions with a conductive gold AFM probe and target molecules covered on the gold/graphene substrates. To obtain the contact between the two electrodes, the AFM contact mode is selected at the scan rate of 1 Hz,

sample bias of 0.3 V and applied piezo scanner voltage of 0.5 V to 8 V (corresponding to a force of 20 to 300 nN). The current amplifier was calibrated using high precision resistors (see SI for more details). The force applied to the surface can be varied depending on the experimental conditions and requirements. In our setup, we use the minimum force which gives a sufficiently stable current signal. Similar to STM based techniques, the collected current and distance signals were then sent for data analysis to get the most probable conductance values of the junction.

3.Results and discussion

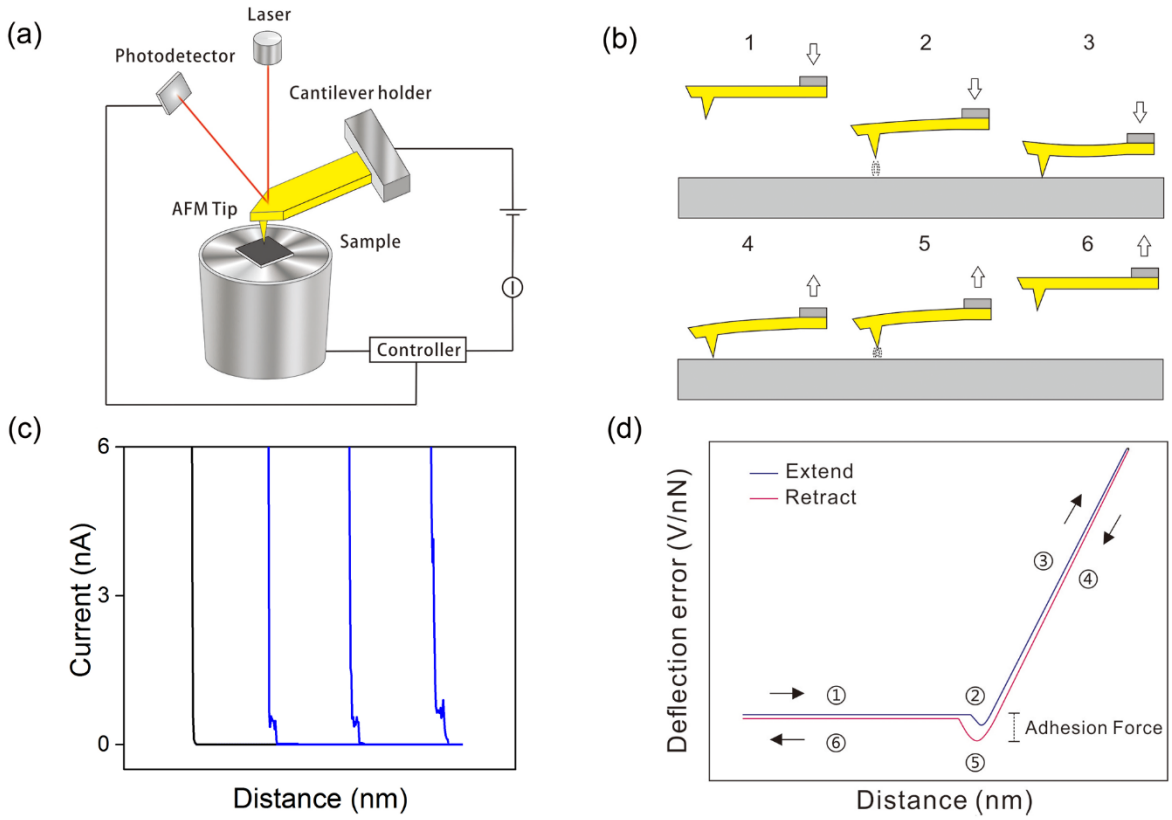

Figure 1. (a) Schematic diagram of the CP-AFM BJ technique. (b) The tip movement of the AFM tip and molecular junctions formed during the process. The AFM probe was firstly brought close to the substrate (1-3) and then withdrawn to its initial distance (4-6) after the contact is established. (c) Typical current-distance curves of bare substrate (black, without molecular junctions formed)

and molecular junctions formed (blue). (d) Typical force-distance curves representing the force loaded on the surface. The arrow and numbers (1-6) correspond to the tip movements in (b). The curves were sketched based on the data from gold-1,8 octanedithiol-gold junctions for better illustration (see Figure S1 for raw data).

We first determined the conductance of gold-1,8 octanedithiol-gold molecular junctions using the three techniques described in the introduction. The detailed setup for STM-based techniques can be either found in our previously studies or other literature.[24-26] A description of the CP-AFM break junction method with the concurrent collection of currents and forces is given in the following text. Instead of using a fixed tip-sample distance while collecting the I-V data, in the CP-AFM BJ technique the current and tip-sample distance is recorded at a fixed bias voltage as the AFM tip-cantilever assembly is rapidly retracted from the surface. Figure 1a shows a schematic diagram of the CP-AFM BJ method. The AFM force feedback circuit is used to control the force applied to the sample, while an extra electrical circuit is used to collect the current signal. Similar to the STM BJ method, the conductive AFM probe was initially set at a given distance and then brought close to the substrate surface until contact is established (position 1-3 in Figure 1b). During the approach process, a jump to contact force is observed (2) followed by a corresponding deflection of the cantilever as it is moved to the set-point force (3). The AFM probe was then withdrawn to its initial distance by adjusting the piezo scanner of the AFM (positions 4-6 in Figure 1b), and a jump from contact is observed at position 5 during the process. The molecular targets can span the narrow gap through the stochastic formation of molecular junctions both during the approach and retraction processes (position 1-2 and 5-6). In such circumstance, a plateau feature is observed during retraction, signifying the formation of a molecular junction (blue curves in Figure 1c). For situations where no molecular junctions formed, a fast decay of the current is

observed as a function of the distance (black curve in Figure 1c). It is noted that the 'distance' here is not the real length of the molecular junction, but the extension or retraction of the piezo scanner. Figure 1d shows a sketched illustrative force-distance curve which shows the loading of the force on the surface and the subsequent cleavage of junction as the piezo scanner is extended. This curve contains information about the force applied to the AFM probe and the adhesion force. In the case of molecular monolayers, it would be expected that a higher force loaded on the surface would produce a greater deformation of the monolayer and possibly a greater contacting footprint both of which may be likely to give a higher junction conductivity. Excessive force may result in the structural damage to probe apex, SAMs and the bottom electrode, therefore careful control and monitoring of the force curve is desirable. It is important to note however the CP-AFM BJ experiments are different to the conventional CP-AFM experiments on molecular monolayers, since in the former case the force is being unloaded as conductance is measured while the tip/cantilever assembly is being retracted. Nevertheless, adhesion force might be important for such determinations.[27] The molecular junction is broken as the AFM probe snaps back from the surface. Forces are negative ("attractive") and in general the magnitude of such forces is about 10 nN according to the literature.[6,27] Another possible source of adhesion is the capacitive force which might be expected to scale with the magnitude of the applied voltage. In most of the situations, this is relatively minor, for example, around 1 nN at a voltage of 1 V.[2]

In our experiment, the movement (deflection) of the probe is achieved by applying the bias voltage to the piezo scanner, an additional conversion of the voltage to the force signal is required in order to plot the force versus distance curve. In the simplest situation in the contact regime the spring constant formula, $F=kx$, can be applied where F is the force applied to the surface, k is the spring constant of the gold probe and x is the deflection of the gold probe (see SI for detailed

explanations). We applied the minimum force (lowest deflection of the probe) to the surface where the current signal is stable. Such contacting force can be varied (from 20 nN to 300 nN) during the process which is highly dependent on the topographical situation of the sample and the SAMs of the molecules.

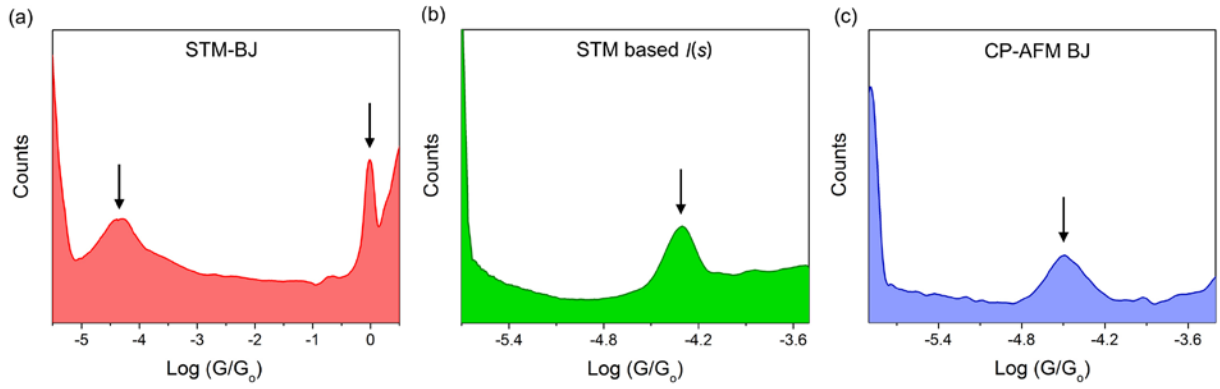

Figure 2. Conductance histograms for gold-1,8 octanedithiol-gold junctions constructed by (a) STM BJ, (b) STM based *I*(*s*) and (c) CP-AFM BJ techniques.

Generally, over 10000 current-distance raw curves were collected with the preset bias voltage and set-point current followed by a data analysis, either manually or automatically. The plateau featuring curves were then used to plot the 1D conductance histogram representing the most probable conductance value of the junction. Figure 2 shows the 1D conductance histograms of gold-1,8 octanedithiol-gold molecular junctions recorded by STM-BJ, STM based *I*(*s*) and CP-AFM BJ techniques, respectively. Two dominant peaks located at 3.5 nS and 77400 nS are observed in the Figure 2a, demarking the most probable conductance value of the molecular junction and gold-gold quantum contact conductance G_o ($G_o=2e^2/h$), respectively. Owing to the limitation of the detector dynamic range, only the conductance peaks located at 3.7 nS and 2.3 nS are observed in Figure 2b and 2c, respectively. The conductance values of the three techniques are in good agreement with previous studies,[28-29] indicating the reliability and stability of our setup.

The conductance value obtained from CP-AFM BJ is slightly lower than from STM based techniques. This may be due to differences in how the contacts are formed and how gold atoms rearrange during the contacting process, resulting in different distribution of favored contacting configurations.[9] During the early stages of single molecule conductance measurement, there was some apparent discrepancies in the literature, with reports of different conductance values for gold-octanedithiol-gold molecular junctions created by different methods.[13-16] In an early report, Chen *et al.* distinguished two sets of peaks, which were designated as high conductance (HC) and low conductance (LC) values.[28] As discussed in a review, and references therein, the different conductance groups could be related to the different molecule-contact morphologies and the roughness of electrode contacts.[16,30] Different conductance groups could be attributed to different possible molecule-electrode configurations; for example, with the sulfur atoms coordinated to either single gold atoms, bonding to multiple surface atoms or in higher coordination defects sites such as at gold steps.[16]

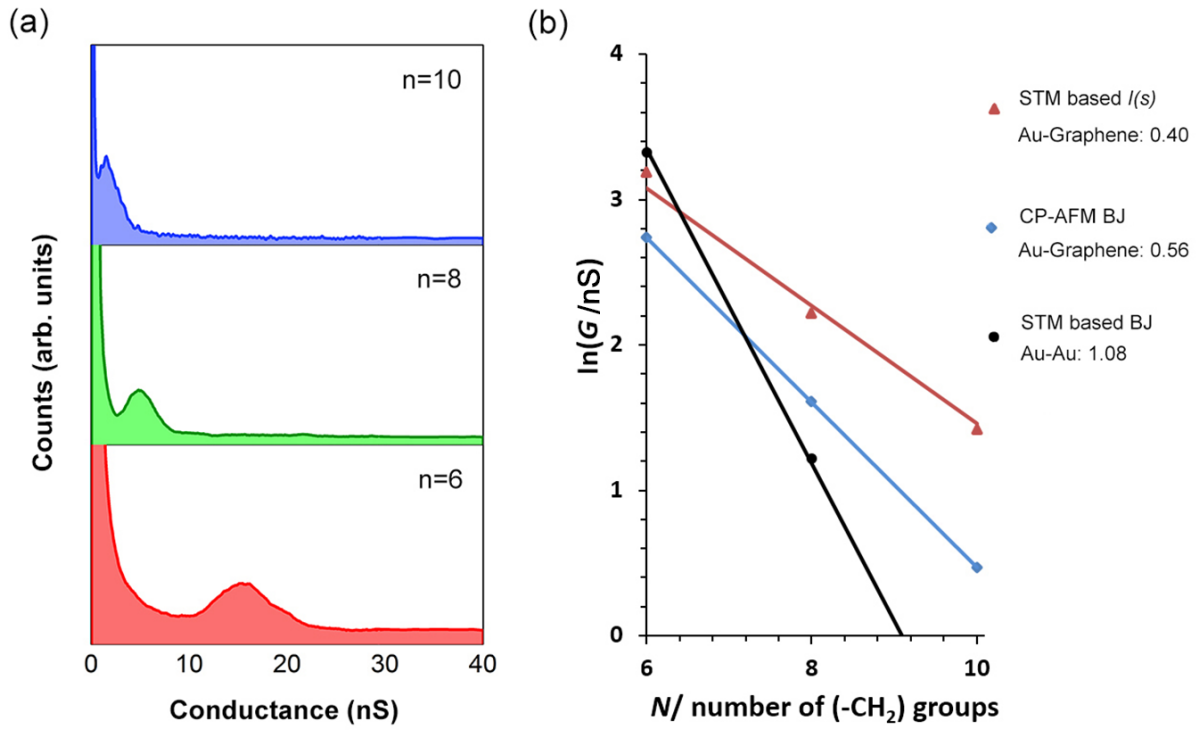

Figure 3. (a) Conductance histograms for gold-n-alkanedithiol-graphene junctions (n = 6, 8, 10). (b) Natural logarithmic plot of the conductance with the number of methylene groups measured by different techniques: red line measured by the STM based *I*(*s*) technique, blue line measured by the CP-AFM BJ method, black line measured by the STM BJ technique.

The bottom gold electrode is now replaced by the graphene substrate, while using the same setup as the described in the foregoing text for gold-1,8 octanedithiol-gold single molecule junctions. The aim here is to investigate the impact for substituting a gold for a graphene contact and whether the junction formation method plays a role. Figure 3a shows stacked 1D histograms of gold-n-alkanedithiol-graphene junctions (n = 6, 8, 10) with the same conductance and counts scale. In each conductance histogram, only one pronounced peak is observed indicating the most probable conductance of the junction. It is clear that the conductance values decrease as a function of the molecular length. In principle a number of approaches might be used to describe the length dependence of the junction conductance,[31] for example, coherent resonant tunneling, coherent non-resonant tunneling or diffusive transport. Here, the transport behavior is typically in the non-resonant tunneling regime, where the conductance scales exponentially with the separation of the electrodes and consequently with the molecular length.[6] Despite its known limitations, it is common to use a simplified Simmons model to express the conductance as G=Aexp(-$\beta_N N$), where β_N is the decay constant, $\beta_N = 2\sqrt{2m\phi/\hbar^2}$,[32-34] and the prefactor A is related to the effective contact resistance which is commonly linked to the nature of the molecule-electrode interaction. To experimentally obtain the decay constant of the junction, the logarithm of the conductance is plotted against the molecular length. Then, the tunneling decay constant, or attenuation factor β_N, is given by the slope of the linear fit and the contact resistance is determined by the intercept at zero junction length.[35] Figure 3b shows the natural logarithmic plot of the conductance with the

number of methylene groups. The blue and red lines represent the decay constant (β_N = 0.56 and 0.40) of gold-alkanedithiol-graphene junctions measured by the CP-AFM BJ technique and the STM based *I*(*s*) technique, respectively. The black line represents the decay constant (β_N = 1.1) of gold-alkanedithiol-gold junctions measured by the STM BJ method from the literature.[28-29] We are not able to measure the conductance of 1,8 octanedithiol with graphene bottom contacts by the STM BJ method using the same experimental setup as shown in Figure 2a. The physical mechanism of forming defined, stable and reproducible metallic contacts by STM BJ method has been well studied by Sabater *et al.* both experimentally and theoretically.[36] They suggested that a clear conductance trace can be obtained when the tip indentation depth is greater than the value which corresponds to a conductance of 5 G_o. This gives a minimum cross section corresponding to 15 atoms for the case of gold. During the contact cycles, a number of gold atoms are exchanged between the two sides of the gold electrode with respect to its original configuration and this tends to reach a constant number after 7-8 cycles. Stable tips are formed after 10 cycles with a pyramidal shape evolving with (111) faces which complies with energetic considerations. Here, in the case of graphene as the bottom electrode, such atoms exchange phenomena between the upper and lower contact are clearly not possible. Since, in the STM BJ method the STM tip is pushed into the substrate, it could be easily compressed or damaged upon hard physical contact with the graphene surface. Therefore, the failure of the STM BJ method to capture a stable current signal with graphene bottom contacts might be explained by the excessive force loaded on the sample. It seems that non-contact STM *I*(*s*) technique or CP-AFM method with in situ force monitoring is more suitable for few layers graphene substrates or other two-dimensional (2D) thin film materials.

Table 1. Conductance values, decay constant and contact resistance for gold-n-alkanedithiol-graphene and gold-n-alkanedithiol-gold junctions (n=6, 8, 10), with literature values included in the latter case. The conductance values involved correspond to the center value of the Gaussian fit from the dominant peak in the conductance histogram.

Molecular junction	Techniques	Conductance (nS)			Decay constant (β_N)	Constant resistance(kΩ)
		n = 6	n = 8	n = 10		
gold-n-alkanedithiol-graphene	CP-AFM break junction (contact mode)	15.6	7.2	1.7	0.56	~ 2100
gold-n-alkanedithiol-graphene	STM based *I*(*s*) (non-contact mode)	24.0	9.0	4.0	0.40[24]	~ 3900
gold-n-alkanedithiol-gold	STM break junction (contact mode)	28.2	3.9	0.2	1.08[28-29]	~ 27

Table 1 summarizes the experimental values as well as the decay constants of non-symmetric gold-n-alkanedithiol-graphene measured by the CP-AFM BJ and STM based *I*(*s*) techniques. The conductance values (LC values in ref. 28 and values in ref. 29) of gold-gold symmetric junctions are also listed for a comparison. The conductance values obtained with the CP-AFM BJ method for graphene bottom contacts are slightly lower than the ones reported in our previous work[24] using the STM based *I*(*s*) technique which may be related to different ways in which the junctions are created. Both CP-AFM BJ and *I*(*s*) techniques show similarly low decay constant (β_N) values for gold-alkanedithiol-graphene junctions when compared to the much higher β_N values for symmetric gold-gold molecular junctions. Our previous experimental and theoretical studies have suggested that the low decay constant is ascribed to the breaking of the junction symmetry.[24-25] Here, in the present case of non-symmetric gold-n-alkanedithiol-graphene junctions constructed by CP-AFM BJ method, we observe the same behavior. It is well known that thiolate can form a strong covalent

bond with gold while the interaction of the thiol with graphene is mainly related to van der Waals (vdW) interaction.[37] The contact resistance is given by extrapolating the chain length to zero in Figure 3b, and the resistance values are found to be ~ 3900 and ~ 2700 kΩ for graphene non-symmetric junctions by formed STM *I*(*s*) and AFM based techniques, respectively. These values can be compared to much lower resistance (~ 27 kΩ) for Au-alkanedithiol-Au symmetrical junctions. This can be explained by the coupling at the graphene-molecule interface which is quite weak and primarily dominated by vdW coupling. The influence of electrode materials on contact resistance in the low-voltage regime has been investigated by the Frisbie group.[38] It was reported in that case that for metallic electrodes the contact resistance decreases substantially with increasing electrode work function. The work function of the single-layer graphene is around 4.5 eV,[39] which is lower than the gold at 5.3 eV,[40] therefore, this is also consistent with a higher contact resistance for Au(tip)/Graphene(substrate) compared to the Au(tip)/Au(substrate) system. Due to the high asymmetry of the junctions the thiol-graphene dipole does not compensate the thiolate-gold dipole and a significant HOMO level shift towards the Fermi level is then observed.[24] This explains why we obtained low decay constant values in both techniques with graphene bottom contacts and reveals that the change of decay values is mainly dependent on the electrode itself and not on the measurement method.

4.Conclusions

In summary, we have used CP-AFM break junction method to study the effects of molecule-electrode contacts in single molecular junctions. The typical gold-octanedithiol-gold molecular junctions fabricated by STM BJ, STM based *I*(*s*) and CP-AFM BJ techniques were firstly examined to verify the stability of the experimental setup and the determined conductance values

agree well with the literature. This setup was then used to investigate the differences which transpire when the bottom electrode contact is changed from a gold to graphene substrate to form gold-n-alkanedithiol-graphene molecular junctions. Both the STM based *I*(*s*) and CP-AFM BJ techniques showed a similar behavior, namely the conductance decays exponentially as a function of the molecular length with β_N of 0.40 and 0.56 for gold-graphene asymmetric junctions. This is significantly lower than the corresponding symmetric Au-alkanedithiol-Au junctions (β_N = 1.1) previously reported in literature. This behavior leads us to suggest that the change of decay values is mainly related to the electrodes itself and not greatly influenced by the measurement method. Both CP-AFM BJ and *I*(*s*) show contact resistance values on the molecule-graphene side that are much higher than that on the molecule-gold side. The resulting unbalanced interactions at these two different sides of the molecular junction results in a non-compensation between thiol-graphene and thiolate-gold dipoles. This consequently leads to a significant HOMO level shift towards the Fermi level, as we have theoretically described in previous publications.[24-25] A slightly lower conductance value measured by the CP-AFM BJ with respect to the STM based *I*(*s*) technique is also observed which may be due to differences in the junction formation method and in the resulting distribution of molecule-electrode contacts. On the other hand, the STM BJ technique does not lead to the formation of stable molecular junctions with graphene bottoms contacts. The STM BJ technique requires that a hard physical contact is made between the tip and substrate, which differs from the STM based *I*(*s*) technique which is a non-contact method. There could be many reasons behind this inability of the STM BJ technique to form stable molecular junctions with a graphene bottom contact. The STM BJ technique relies on the formation of gold atomic point contacts which after cleavage form an open Au-Au electrode gap into which molecules can be bound. The pressing of the gold tip onto the graphene substrate will clearly deform the soft gold

apex but may also produce (transient) substrate deformation. A possible reason for the STM BJ technique being ineffective here could be that there is a high transient instability in the gold tip contact after it has been pushed onto the graphene surface and then withdrawn. This highlights that the method for single molecule junction formation be to selected depends on the specific system, notably the respective contact materials.

ASSOCIATED CONTENT

Supporting Information. The Supporting Information is available free of charge on the ACS Publications website at DOIXXXX: Raw data used for plotting current and distance curves, the CP-AFM application module calibration, the standard I-V calibration curve, and explanations for converting applied voltage (V) to corresponded force (F).

AUTHOR INFORMATION

Corresponding Author

*E-mail: li.yang@xjtlu.edu.cn.

Author Contributions

Qian Zhang carried out the main experiments and wrote the first draft of the manuscript. Li Yang, Yannick J. Dappe and Richard J. Nichols designed experiments and wrote the manuscript; Shuhui Tao and Yinqi Fan conducted other complementary experiments; Cezhou Zhao, Chun Zhao and Weitao Su analyzed experimental results. All authors have given approval to the final version of the manuscript.

Notes

The authors declare no competing financial interest.

ACKNOWLEDGMENT

We acknowledge the financial supports by National Natural Science Foundation of China (NSFC Grants 21750110441, 21503169), Suzhou Industrial Park Initiative Platform Development for Suzhou Municipal Key Lab for New Energy Technology (RR0140), Key Program Special Fund in XJTLU (KSF-A-04 and KSF-A-07) and the XJTLU Research Development Fund (PGRS-13-01-03, RDF-14-02-42 and RDF-16-01-33).

REFERENCES

1. Wang, G.; Kim, T. W.; Jo, G.; Lee, T. Enhancement of Field Emission Transport by Molecular Tilt Configuration in Metal−Molecule−Metal Junctions. *J. Am. Chem. Soc.* **2009**, *131*, 5980-5985.

2. Mativetsky, J. M.; Palma, M.; Samori, P. Exploring Electronic Transport in Molecular Junctions by Conducting Atomic Force Microscopy. *Top. Curr. Chem.* **2008**, *285*, 157-202.

3. Reed, M. A.; Zhou, C.; Muller, C. J.; Burgin, T. P.; Tour, J. M. Conductance of a Molecular Junction. *Science* **1997**, *278*, 252-254.

4. Xu, B.; Tao, N. J. Measurement of Single-Molecule Resistance by Repeated Formation of Molecular Junctions. *Science* **2003**, *301*, 1221-1223.

5. Haiss, W.; van Zalinge, H.; Higgins, S. J.; Bethell, D.; Höbenreich, H.; Schiffrin, D. J.; Nichols, R. J. Redox State Dependence of Single Molecule Conductivity. *J. Am. Chem. Soc.* **2003**, *125*, 15294-15295.

6. Wold, D. J.; Frisbie, C. D. Fabrication and Characterization of Metal−Molecule−Metal Junctions by Conducting Probe Atomic Force Microscopy. *J. Am. Chem. Soc.* **2001**, *123*, 5549-5556.

7. Cui, X. D.; Primak, A.; Zarate, X.; Tomfohr, J.; Sankey, O. F.; Moore, A. L.; Moore, T. A.; Gust, D.; Harris, G.; Lindsay, S. M. Reproducible Measurement of Single-Molecule Conductivity. *Science* **2001**, *294*, 571-574.

8. Osorio, H. M.; Martín, S.; López, M. C.; Marqués-González, S.; Higgins, S. J.; Nichols, R. J.; Low, P. J.; Cea, P. Electrical Characterization of Single Molecule and Langmuir–Blodgett Monomolecular Films of a Pyridine-Terminated Oligo(phenylene-ethynylene) Derivative. *Beilstein J Nanotechnol* **2015**, *6*, 1145-1157.

9. Morita, T.; Lindsay, S. Determination of Single Molecule Conductances of Alkanedithiols by Conducting-Atomic Force Microscopy with Large Gold Nanoparticles. *J. Am. Chem. Soc.* **2007**, *129*, 7262-7263.

10. Xu, B.; Xiao, X.; Tao, N. J. Measurements of Single-Molecule Electromechanical Properties. *J. Am. Chem. Soc.* **2003**, *125*, 16164-16165.

11. Huang; Xu; Chen; Ventra, M. D.; Tao. Measurement of Current-Induced Local Heating in a Single Molecule Junction. *Nano Lett.* **2006**, *6*, 1240-1244.

12. Haiss, W.; Nichols, R. J.; van Zalinge, H.; Higgins, S. J.; Bethell, D.; Schiffrin, D. J. Measurement of Single Molecule Conductivity Using the Spontaneous Formation of Molecular Wires. *Phys. Chem. Chem. Phys.* **2004**, *6*, 4330-4337.

13. Li, X.; He, J.; Hihath, J.; Xu, B.; Lindsay, S. M.; Tao, N. Conductance of Single Alkanedithiols: Conduction Mechanism and Effect of Molecule−Electrode Contacts. *J. Am. Chem. Soc.* **2006**, *128*, 2135-2141.

14. Haiss, W.; Martín, S.; Leary, E.; Zalinge, H. v.; Higgins, S. J.; Bouffier, L.; Nichols, R. J. Impact of Junction Formation Method and Surface Roughness on Single Molecule Conductance. *J. Phys. Chem. C* **2009**, *113*, 5823-5833.

15. Li, C.; Pobelov, I.; Wandlowski, T.; Bagrets, A.; Arnold, A.; Evers, F. Charge Transport in Single Au | Alkanedithiol | Au Junctions: Coordination Geometries and Conformational Degrees of Freedom. *J. Am. Chem. Soc.* **2008**, *130*, 318-326.

16. Nichols, R. J.; Haiss, W.; Higgins, S. J.; Leary, E.; Martin, S.; Bethell, D. The Experimental Determination of the Conductance of Single Molecules. *Phys. Chem. Chem. Phys.* **2010**, *12*, 2801-2815.

17. Kelley, T. W.; Granstrom, E.; Frisbie, C. D. Conducting Probe Atomic Force Microscopy: A Characterization Tool for Molecular Electronics. *Adv. Mater.* **1999**, *11*, 261-264.

18. Jia, C.; Guo, X. Molecule-Electrode Interfaces in Molecular Electronic Devices. *Chem. Soc. Rev.* **2013**, *42*, 5642-5660.

19. Kiguchi, M.; Miura, S.; Takahashi, T.; Hara, K.; Sawamura, M.; Murakoshi, K. Conductance of Single 1,4-Benzenediamine Molecule Bridging between Au and Pt Electrodes. *J. Phys. Chem. C* **2008**, *112*, 13349-13352.

20. Nakazumi, T.; Kaneko, S.; Kiguchi, M. Electron Transport Properties of Au, Ag, and Cu Atomic Contacts in a Hydrogen Environment. *J. Phys. Chem. C* **2014**, *118*, 7489-7493.

21. Castellanos-Gomez, A.; Bilan, S.; Zotti, L. A.; Arroyo, C. R.; Agraït, N.; Carlos Cuevas, J.; Rubio-Bollinger, G. Carbon Tips as Electrodes for Single-Molecule Junctions. *Appl. Phys. Lett.* **2011**, *99*, 123105.

22. Song, X.; Hu, J.; Zeng, H. Single Molecule Electronic Devices. *J. Mater. Chem. C* **2013**, *1*, 2952-2969.

23. Ren, B.; Picardi, G.; Pettinger, B. Preparation of Gold Tips Suitable for Tip-enhanced Raman Spectroscopy and Light Emission by Electrochemical Etching. *Rev. Sci. Instrum.* **2004**, *75*, 837.

24. Zhang, Q.; Liu, L.; Tao, S.; Wang, C.; Zhao, C.; González, C.; Dappe, Y. J.; Nichols, R. J.; Yang, L. Graphene as a Promising Electrode for Low-Current Attenuation in Nonsymmetric Molecular Junctions. *Nano Lett.* **2016**, *16*, 6534-6540.

25. Zhang, Q.; Tao, S.; Yi, R.; He, C.; Zhao, C.; Su, W.; Smogunov, A.; Dappe, Y. J.; Nichols, R. J.; Yang, L. Symmetry Effects on Attenuation Factors in Graphene-Based Molecular Junctions. *J. Phys. Chem. Lett.* **2017**, *8*, 5987-5992

26. Venkataraman, L.; Klare, J. E.; Nuckolls, C.; Hybertsen, M. S.; Steigerwald, M. L. Dependence of Single-molecule Junction Conductance on Molecular Conformation. *Nature* **2006**, *442*, 904-907.

27. Engelkes, V. B.; Beebe, J. M.; Frisbie, C. D. Analysis of the Causes of Variance in Resistance Measurements on Metal−Molecule−Metal Junctions Formed by Conducting-Probe Atomic Force Microscopy. *J. Phys. Chem. B* **2005**, *109*, 16801-16810.

28. Chen, F.; Li, X.; Hihath, J.; Huang, Z.; Tao, N. Effect of Anchoring Groups on Single-Molecule Conductance: Comparative Study of Thiol-, Amine-, and Carboxylic-Acid-Terminated Molecules. *J. Am. Chem. Soc.* **2006**, *128*, 15874-15881.

29. Jang, S. Y.; Reddy, P.; Majumdar, A.; Segalman, R. A. Interpretation of Stochastic Events in Single Molecule Conductance Measurements. *Nano Lett.* **2006**, *6*, 2362-2367.

30. Kim, C. M.; Bechhoefer, J. Conductive Probe AFM Study of Pt-Thiol and Au-Thiol Contacts in Metal-Molecule-Metal Systems. *J. Chem. Phys.* **2013**, *138*, 014707.

31. Ratner, M. A.; Davis, B.; Kemp, M.; Mujica, V.; Roitberg, A.; Yaliraki, S. Molecular Wires: Charge Transport, Mechanisms, and Control. *Ann. N.Y. Acad. Sci.* **1998**, *852*, 22-37

32. Engelkes, V. B.; Beebe, J. M.; Frisbie, C. D. Length-Dependent Transport in Molecular Junctions Based on SAMs of Alkanethiols and Alkanedithiols: Effect of Metal Work Function and Applied Bias on Tunneling Efficiency and Contact Resistance. *J. Am. Chem. Soc.* **2004**, *126*, 14287-14296.

33. Cuevas, J. C.; Scheer, E. *Molecular Electronics: An Introduction to Theory and Experiment*; World Scientific: Singapore, 2010.

34. Wang, Y. H.; Zhou, X. Y.; Sun, Y. Y.; Han, D.; Zheng, J. F.; Niu, Z. J.; Zhou, X. S. Conductance Measurement of Carboxylic Acids Binding to Palladium Nanoclusters by Electrochemical Jump-to-contact STM Break Junction. *Electrochim. Acta* **2014**, *123*, 205-210

35. Kim, T.; Liu, Z. F.; Lee, C.; Neaton, J. B.; Venkataraman, L. Charge Transport and Rectification in Molecular Junctions Formed with Carbon-based Electrodes. *Proc. Natl. Acad. Sci. U. S. A.* **2014**, *111*, 10928-10932.

36. Sabater, C.; Untiedt, C.; Palacios, J. J.; Caturla, M. J. Mechanical Annealing of Metallic Electrodes at the Atomic Scale. *Phys. Rev. Lett.* **2012**, *108*, 205502.

37. Adak, O.; Kladnik, G.; Bavdek, G.; Cossaro, A.; Morgante, A.; Cvetko, D.; Venkataraman, L. Ultrafast Bidirectional Charge Transport and Electron Decoherence at Molecule/Surface Interfaces: A Comparison of Gold, Graphene, and Graphene Nanoribbon Surfaces. *Nano Lett.* **2015**, *15*, 8316-8321.

38. Beebe, J. M.; Engelkes, V. B.; Miller, L. L.; Frisbie, C. D. Contact Resistance in Metal−Molecule−Metal Junctions Based on Aliphatic SAMs: Effects of Surface Linker and Metal Work Function. *J. Am. Chem. Soc.* **2002**, *124*, 11268-11269.

39. Liang, S. J.; Ang, L. K. Electron Thermionic Emission from Graphene and a Thermionic Energy Converter. *Phys. Rev. Applied* **2015**, *3*, 014002

40. Sachtler, W. M. H.; Dorgelo, G. J. H.; Holscher, A. A. The Work Function of Gold. Surface. *Science* **1966**, *5*, 221-229.

TOC Graphic

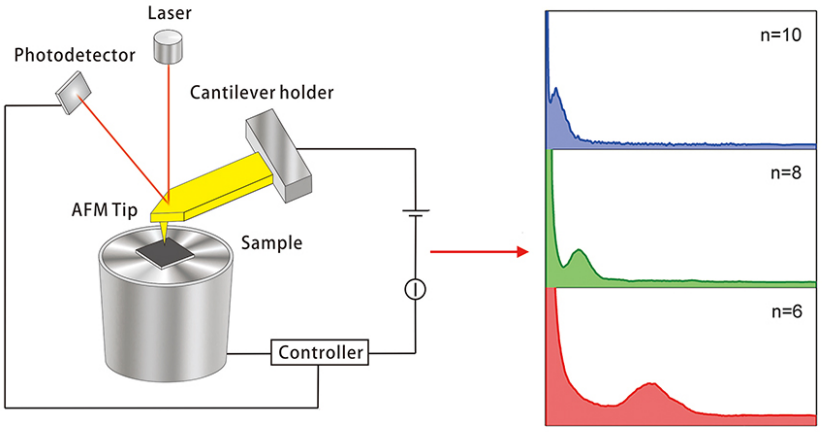

CP-AFM BJ technique

Conductance histogram